

Contents lists available at [SciVerse ScienceDirect](http://SciVerse.Sciencedirect.com)

# Biochimica et Biophysica Acta

journal homepage: [www.elsevier.com/locate/bbambio](http://www.elsevier.com/locate/bbambio)

## The contribution of thioredoxin-2 reductase and glutathione peroxidase to H<sub>2</sub>O<sub>2</sub> detoxification of rat brain mitochondria <sup>☆</sup>

Alexei P. Kudin <sup>a,b</sup>, Bartłomiej Augustynek <sup>a,b,c</sup>, Anja Kerstin Lehmann <sup>d</sup>,  
Richard Kovács <sup>d</sup>, Wolfram S. Kunz <sup>a,b,\*</sup>

<sup>a</sup> Department of Epileptology, University of Bonn, Sigmund-Freud-Str. 25, D-53105 Bonn, Germany

<sup>b</sup> Life & Brain Center, University of Bonn, Sigmund-Freud-Str. 25, D-53105 Bonn, Germany

<sup>c</sup> Laboratory of Intracellular Ion Channels, Nencki Institute of Experimental Biology, 3 Pasteur St., 02-093 Warsaw, Poland

<sup>d</sup> Institute for Neurophysiology, Charité-Universitätsmedizin Berlin, Oudenarder Str. 16, D-13347 Berlin, Germany

### ARTICLE INFO

#### Article history:

Received 2 December 2011

Received in revised form 17 February 2012

Accepted 21 February 2012

Available online 28 February 2012

#### Keywords:

Rat brain mitochondria

Hydrogen peroxide metabolism

Thioredoxin-2 reductase

Glutathione peroxidase

### ABSTRACT

Brain mitochondria are not only major producers of reactive oxygen species but they also considerably contribute to the removal of toxic hydrogen peroxide by the glutathione (GSH) and thioredoxin-2 (Trx2) antioxidant systems. In this work we estimated the relative contribution of both systems and catalase to the removal of intrinsically produced hydrogen peroxide (H<sub>2</sub>O<sub>2</sub>) by rat brain mitochondria. By using the specific inhibitors auranofin and 1-chloro-2,4-dinitrobenzene (DNCB), the contribution of Trx2- and GSH-systems to reactive oxygen species (ROS) detoxification in rat brain mitochondria was determined to be 60 ± 20% and 20 ± 15%, respectively. Catalase contributed to a non-significant extent only, as revealed by aminotriazole inhibition. In digitonin-treated rat hippocampal homogenates inhibition of Trx2- and GSH-systems affected mitochondrial hydrogen peroxide production rates to a much higher extent than the endogenous extramitochondrial hydrogen peroxide production, pointing to a strong compartmentation of ROS metabolism. Imaging experiments of hippocampal slice cultures showed on single cell level substantial heterogeneity of hydrogen peroxide detoxification reactions. The strongest effects of inhibition of hydrogen peroxide removal by auranofin or DNCB were detected in putative interneurons and microglial cells, while pyramidal cells and astrocytes showed lower effects. Thus, our data underline the important contribution of the Trx2-system to hydrogen peroxide detoxification in rat hippocampus. This article is part of a Special Issue entitled: 17th European Bioenergetics Conference (EBEC 2012).

© 2012 Elsevier B.V. All rights reserved.

### 1. Introduction

Reactive oxygen species (ROS) are formed by one electron transfer of reducing equivalents to molecular oxygen. In brain tissue a considerable part is generated by mitochondrial respiratory chain [1] at respiratory chain complexes I and III. Subsequent rapid dismutation of O<sub>2</sub> by Mn superoxide dismutase (MnSOD) generates the more stable hydrogen peroxide (H<sub>2</sub>O<sub>2</sub>) in the mitochondrial matrix, which can, in turn, affect cell function by reacting with thiol residues in redox-sensitive proteins either within the mitochondria or in the cytoplasm

(if exported through aquaporin 9 [2]). Alternatively, it can form the very reactive OH<sup>•</sup> radical by Fenton reaction. Under redox balanced conditions, mitochondrial H<sub>2</sub>O<sub>2</sub> production is offset by the scavenging capacity of the GSH and thioredoxin-2 (Trx2) antioxidant systems. The Trx2- and GSH-systems buffer H<sub>2</sub>O<sub>2</sub> via peroxiredoxin-3 (Prx3) [3,4] and glutathione peroxidase-1 and -4 [5], respectively. The other H<sub>2</sub>O<sub>2</sub> scavenger, catalase, is present only at very low amounts in brain [6] and heart mitochondria [7], but very abundant in liver mitochondria [8]. Both GSH and Trx2 require a continuous supply of NADPH-dependent reducing equivalents from GSH reductase and mitochondrial thioredoxin reductase-2 (TrxR2) [9–12]. There is ample evidence indicating that both systems are non-redundant and that the flow of electrons through each system is independently regulated [13,14]. In the present study we used the specific inhibitors of Trx2 and GSH antioxidant systems auranofin and DNCB as well as the catalase inhibitor aminotriazole to evaluate the relative contribution of the individual systems to hydrogen peroxide detoxification in rat brain mitochondria, rat hippocampal homogenates and rat hippocampal slice cultures.

**Abbreviations:** ROS, reactive oxygen species; Trx2, thioredoxin-2; GSH, glutathione; SOD, superoxide dismutase; DNCB, 1-chloro-2,4-dinitrobenzene; L-GP, L-α-glycerophosphate

<sup>☆</sup> This article is part of a Special Issue entitled: 17th European Bioenergetics Conference (EBEC 2012).

\* Corresponding author at: Division of Neurochemistry, Department of Epileptology, University Bonn Medical Center, Sigmund-Freud-Str. 25, D-53105 Bonn, Germany. Tel.: +49 228 6885 290; fax: +49 228 6885 236.

E-mail address: [wolfram.kunz@ukb.uni-bonn.de](mailto:wolfram.kunz@ukb.uni-bonn.de) (W.S. Kunz).

## 2. Materials and methods

### 2.1. Solutions

In the experiments described here the following solutions were used: MSE solution (for homogenate and mitochondria isolation) containing 225 mM mannitol, 75 mM sucrose, 1 mM EGTA, 5 mM HEPES, and 1 mg/ml essential fatty acid free BSA (pH 7.4); and MTP medium (standard measurement medium) containing 10 mM  $\text{KH}_2\text{PO}_4$ , 60 mM KCl, 60 mM Tris-HCl, 110 mM mannitol, 5 mM  $\text{MgCl}_2$  and 0.5 mM EDTA (pH 7.4).

### 2.2. Homogenate preparation and isolation of mitochondria

The investigated rat hippocampal homogenates ( $n=10$ ) were prepared according to the following procedure. A male Wistar II rat (~50 days old) was euthanized, and the brain was rapidly removed. The rat hippocampus tissue was washed and immediately placed into ice-cold MSE medium. About 100 mg wet tissue was homogenized twice for 20 s at 8000 rpm using an ultra-turrax homogenizer T 25 (IKA, Staufen, Germany) in 0.5 ml ice cold MSE medium.

Rat brain mitochondria were isolated according to the protocol originally described by Rosenthal et al. [15] with small modification that allowed to obtain mitochondria with much better functional characteristics [16]. The respiratory control index with 10 mM glutamate and 5 mM malate as respiratory substrates was with all preparations routinely better than 5; the specific active state respiration rate of rat brain mitochondria was  $210 \pm 7$  nmol  $\text{O}_2$ /min/mg protein ( $n=4$ ).

### 2.3. Measurement of $\text{H}_2\text{O}_2$ generation

$\text{H}_2\text{O}_2$  generation was measured with the Amplex Red/peroxidase-coupled method (1  $\mu\text{M}$  Amplex Red ( $\lambda_{\text{ex}} = 560$  nm,  $\lambda_{\text{em}} = 590$  nm) + 20 units/ml horseradish peroxidase in the additional presence of 30 units/ml SOD).

All measurements of ROS generation were performed at 30 °C in oxygen-saturated MTP medium 60 mM KCl, pH 7.4 [1]. The fluorescent signal was calibrated by known  $\text{H}_2\text{O}_2$  concentrations in the absence/presence of inhibitors applied. In the calculations of quantitative  $\text{H}_2\text{O}_2$  generation rates catalase-insensitive Amplex Red oxidation rates were always subtracted.

### 2.4. Slice cultures

Slice cultures were prepared and maintained according to the Stoppini method [17]. Seven days old Wistar rats were decapitated, the brains were removed and submerged in ice-cold gassed (95%  $\text{O}_2$ , 5%  $\text{CO}_2$ ) minimal essential medium (MEM). Hippocampal slices (400  $\mu\text{m}$ , McIlwain Tissue Chopper, Mickle Laboratories, Guildford, UK) were cut and placed on a culture plate insert (MilliCell-CM, Millipore, Eschborn, Germany). Culture medium (containing: 50% MEM, 25% Hank's Balanced Salt Solution, 25% Horse Serum, pH 7.4; Gibco, Eggenstein, Germany) was replaced three times a week. Slice cultures were used for experiments after 6 to 11 days in vitro.

### 2.5. Fluorescence imaging

Slice cultures were incubated with a combination of MitoSox, (5  $\mu\text{M}$ ) and 2',7'-dichlorodihydrofluorescein diacetate ( $\text{H}_2\text{DCFDA}$ , 20  $\mu\text{M}$ , 60–120 min) in the incubator at 36 °C and moved to the recording chamber mounted on an epifluorescent microscope (Olympus BX51WI, Olympus-Europe GmbH, Hamburg). The chamber was superfused with gassed ACSF (5 ml/min, 30 °C), containing (in mM): NaCl 129, KCl 3,  $\text{NaH}_2\text{PO}_4$  1.25,  $\text{MgSO}_4$  1.8,  $\text{CaCl}_2$  1.6,  $\text{NaHCO}_3$

26 and glucose 10 (pH 7.4).  $\text{H}_2\text{DCFDA}$  (2  $\mu\text{M}$ ) was added to the perfusion during the whole duration of the experiment.

Fluorescence recordings were performed with a spinning disk confocal microscope (Andor Revolution, BFOptilas GmbH, Gröbenzell, Germany). Fluorescence from the CA3 region of the hippocampus was obtained by a 20 $\times$  water immersion objective (N.A.: 0.3). In order to minimize photo-bleaching and interaction of illumination with free radical formation, exposure time was kept short (120 ms) and acquisition rate for time series reduced to one z-scan per 40 s. In order to reconstruct the upper ~60  $\mu\text{m}$  of the CA3 area 18–21 z-planes were obtained (3  $\mu\text{m}$  steps) for each time point by using a fast-piezo z-scanner (Physik Instrumente, Berlin, Germany). After a 10 min recording of the fluorescence baseline auranofin (5–10  $\mu\text{M}$ ) or DNCB (50  $\mu\text{M}$ ) was added to the perfusion and fluorescence monitored for additional 30 min.

Data evaluation and 3D reconstruction were carried out with the acquisition software Andor IQ (BFOptilas GmbH, Gröbenzell, Germany) and with ImageJ (Wayne Rasband, NIH, USA). For each time point a maximum intensity projection of the z-scans was created and changes in fluorescence were evaluated for each fluorescence channel in manually delineated regions of interests (ROI). Fluorescence is given as  $\Delta f/f_0$  in percent where  $f_0$  represents the average fluorescence from the first 2 min of a recording.

## 3. Results

### 3.1. Auranofin and DNCB stimulate $\text{H}_2\text{O}_2$ production in isolated rat brain mitochondria

In Fig. 1 the effects of inhibition of  $\text{H}_2\text{O}_2$  removal by the Trx2- (auranofin) and the GSH-systems (DNCB) on reverse electron transport-driven  $\text{H}_2\text{O}_2$  production from succinate are presented.

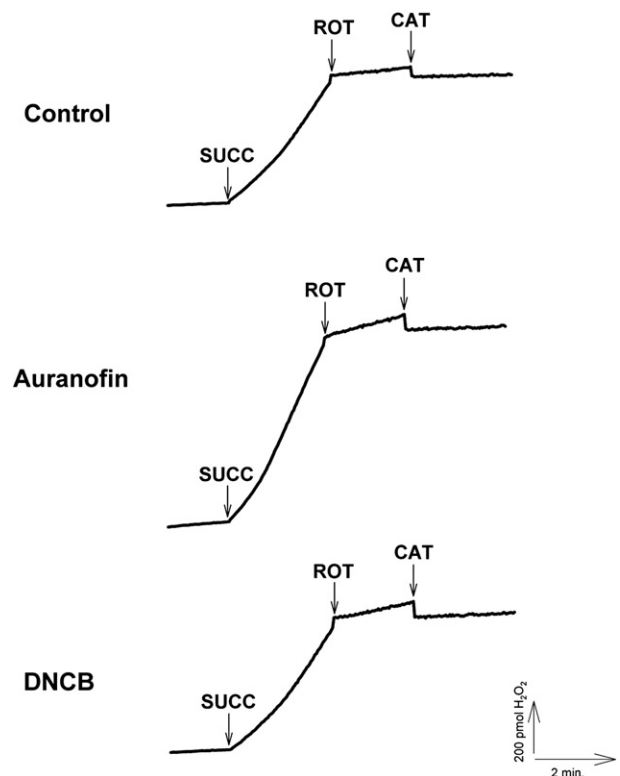


**Fig. 1.** Effect of auranofin and DNCB on reverse electron transport-driven  $\text{H}_2\text{O}_2$  generation. Experimental traces of Amplex Red fluorescence changes observed in rat brain mitochondria (0.1 mg protein/ml) in the absence (Control) or in the presence of 1  $\mu\text{M}$  auranofin (Auranofin) or 10  $\mu\text{M}$  DNCB (DNCB). The arrows indicate the addition of 10 mM succinate (SUCC), 6.7  $\mu\text{M}$  rotenone (ROT) and catalase (CAT, 12000 units/ml).

Under these circumstances, hydrogen peroxide is formed by matrix-localized MnSOD from superoxide formed at the FMN moiety of respiratory chain complex I [16]. Very clearly, both inhibitors of the Trx2- and GSH-systems stimulated the Amplex Red detectable  $H_2O_2$  production of brain mitochondria nearly 2-fold. On the other hand the effect of catalase inhibition by 2 mM aminotriazole was negligibly small (data not shown). A similar stimulation is visible if the ROS generation by forward electron transfer is measured (Fig. 2). Here, glutamate and malate were used as respiratory substrates and rotenone as an inhibitor of complex I, which stimulated ROS production at the very same site as under conditions of reverse electron transport [16]. To test the possible effects of localization of the ROS producing site we used  $\alpha$ -glycerophosphate as mitochondrial substrate (Fig. 3). This substrate leads to a more pronounced ROS generation than glutamate and malate, which is partially sensitive to rotenone. This indicates that at least a part of this ROS generation can be explained by reverse electron transport. Antimycin addition caused a very prominent ROS production, comparable to the reverse electron transport-driven ROS production with succinate as substrate (cf. Fig. 1). Under all investigated conditions the stimulating effects of auranofin and DNCB on ROS production were clearly detectable, being always more pronounced with auranofin.

In separate experiments we have tested the concentration dependencies and the potential dependence of the inhibitory effects of auranofin and DNCB. The concentration dependencies are shown in Fig. 4A and B. For auranofin a  $I_{50}$  value of 0.01  $\mu$ M was determined (Fig. 4A), while the  $I_{50}$  value for DNCB was 2  $\mu$ M (Fig. 4B). Furthermore, we have tested the effects of the less specific compound DNCB on thioredoxin reductase activity of isolated rat brain mitochondria. Up to a concentration of 20  $\mu$ M DNCB the activity of thioredoxin

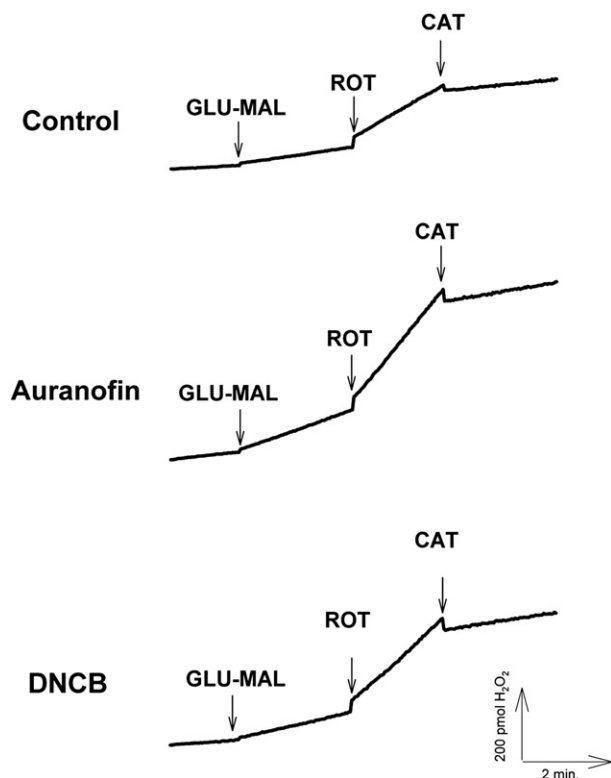


**Fig. 2.** Effect of auranofin and DNCB on direct electron flow-driven  $H_2O_2$  generation. Experimental traces of Amplex Red fluorescence changes observed in rat brain mitochondria (0.1 mg protein/ml) in the absence (Control) or in the presence of 1  $\mu$ M auranofin (Auranofin) or 10  $\mu$ M DNCB (DNCB). The arrows indicate the addition of 10 mM glutamate and 5 mM malate (GLU-MAL), 6.7  $\mu$ M rotenone (ROT) and catalase (CAT, 12000 units/ml).

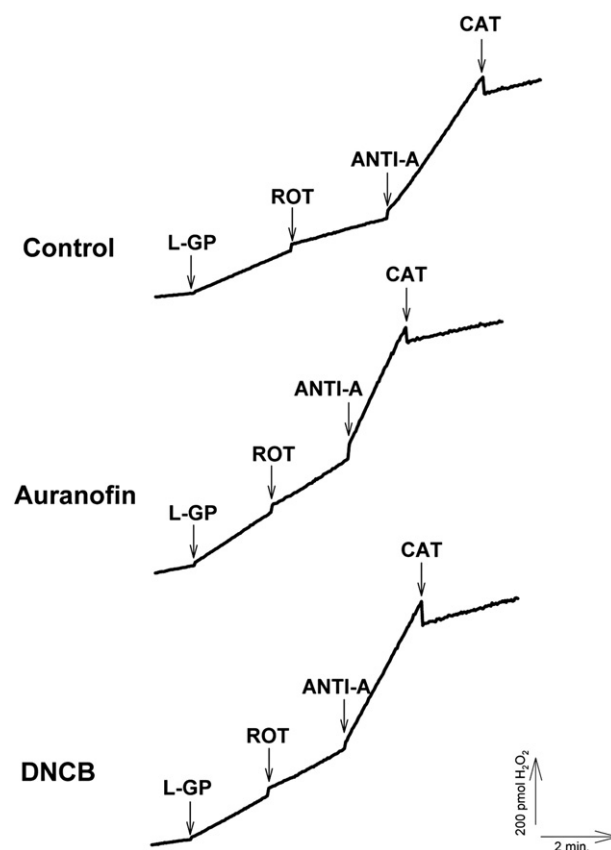


**Fig. 3.** Effect of auranofin and DNCB on glycerophosphate-driven  $H_2O_2$  generation. Experimental traces of Amplex Red fluorescence changes observed in rat brain mitochondria (0.1 mg protein/ml) in the absence (Control) or in the presence of 1  $\mu$ M Auranofin (Auranofin) or 10  $\mu$ M DNCB (DNCB). The arrows indicate the addition of 10 mM L- $\alpha$ -glycerophosphate (L-GP), 6.7  $\mu$ M rotenone (ROT), 0.5  $\mu$ M antimycin A (ANTI-A) and catalase (CAT, 12000 units/ml).

reductase remained nearly unaffected (3 independent experiments, data not shown, cf. [20]).

Table 1 summarizes the quantitative values of hydrogen peroxide generation rates of rat brain mitochondria in the presence of different inhibitors and substrates. Importantly, the stimulating effects of auranofin and DNCB were in all experimental conditions additive. When the data from all experimental conditions are averaged, the relative contribution of the auranofin-sensitive hydrogen peroxide detoxification reaction was  $60 \pm 20\%$  and of DNCB-sensitive hydrogen peroxide detoxification reaction was  $20 \pm 15\%$ .

### 3.2. Auranofin and DNCB stimulate mitochondrial hydrogen peroxide production in rat hippocampal homogenates

To estimate the contribution of different cellular compartments in tissue hydrogen peroxide generation (cf. [1]), we determined the effects of auranofin and DNCB on stimulation of hydrogen peroxide generation rates in digitonin-permeabilized rat hippocampal homogenates. The experimental data are summarized in Table 2. Interestingly, a relatively high endogenous hydrogen peroxide generation rate was noticed, which was neither enhanced by auranofin nor by DNCB nor by aminotriazole, but stimulated by digitonin permeabilization. On the other hand, auranofin and DNCB substantially stimulated specifically mitochondrial hydrogen peroxide synthesis, which was especially visible in the presence of succinate, glutamate + malate + rotenone,  $\alpha$ -glycerophosphate and  $\alpha$ -glycerophosphate + rotenone + antimycin. Under these conditions the addition of 2 mM aminotriazole was without any measurable effect (data not shown),

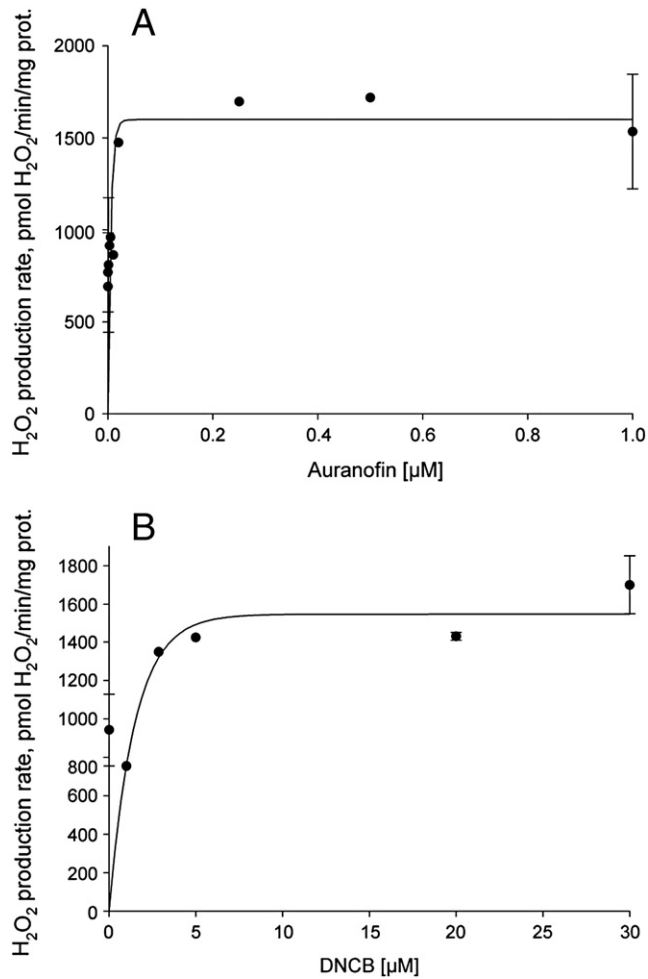


**Fig. 4.** Dependency of  $H_2O_2$  generation rate in the presence of glutamate + malate and rotenone on auranofin (A) and DNCB (B) concentrations.  $H_2O_2$  generation rate was measured with Amplex Red-based method in the presence of SOD (30 U/ml) and 10 mM glutamate + 5 mM malate and 6.7  $\mu$ M rotenone. The quantitative data are presented as average values of 4 independent mitochondrial preparations.

which is a strong indication that only the Trx2- and GSH-systems utilize the mitochondrially produced hydrogen peroxide.

### 3.3. The contribution of the Trx2- and GSH-systems to antioxidant defense in rat hippocampal slice cultures

In order to investigate the contribution of Trx2- and GSH-systems to the antioxidant defense of neuronal tissue in situ, we applied

**Table 1**

Rates of hydrogen peroxide production of isolated rat brain mitochondria in the presence of inhibitors of Trx2- and GSH-systems.

	Control	Auranofin	CDNB	Aura + CDNB
Succinate	2565 ± 772	2884 ± 615	2374 ± 416	2860 ± 520
Succ + Rot	169 ± 34	381 ± 62	259 ± 76	583 ± 92
Succ + Rot + Anti	387 ± 87	650 ± 154	560 ± 66	910 ± 195
Glut + Mal	84 ± 33	287 ± 54	141 ± 31	445 ± 86
Glut + Mal + Rot	779 ± 243	1324 ± 244	1155 ± 210	1757 ± 257
L-glycero-phosphate	141 ± 77	400 ± 92	202 ± 66	503 ± 79
L-GP + Rot	0 ± 41	226 ± 94	122 ± 97	462 ± 87
L-GP + Rot + Anti	1520 ± 358	1715 ± 324	1524 ± 378	2004 ± 326

The data are averages of 6 independent mitochondrial preparations ± SD and expressed in pmol  $H_2O_2$ /min/mg protein. Experimental conditions as presented in Figs. 1, 2 and 3.

Please note, that an endogenous catalase-sensitive Amplex Red oxidation rate was not detected.

**Table 2**

Rates of hydrogen peroxide production of rat hippocampal homogenates in the presence of inhibitors of Trx2- and GSH-systems.

	Control	Auranofin	CDNB	Aura + CDNB
Endogenous rate <sup>a</sup>	314 ± 94	329 ± 90	264 ± 56	309 ± 73
Endogenous rate after digitonin treatment <sup>a</sup>	418 ± 123	440 ± 136	388 ± 95	436 ± 88
Succinate	606 ± 188	729 ± 185	624 ± 179	797 ± 202
Succ + TTFB	317 ± 64	391 ± 132	336 ± 55	367 ± 82
Succ + TTFB + Anti	356 ± 73	407 ± 93	364 ± 62	400 ± 113
Glut + Mal	436 ± 155	449 ± 153	469 ± 143	518 ± 157
Glut + Mal + Rot	502 ± 186	551 ± 168	580 ± 195	660 ± 202
L-glycerophosphate	563 ± 161	642 ± 104	529 ± 145	654 ± 128
L-GP + Rot	420 ± 113	499 ± 75	406 ± 124	502 ± 84
L-GP + Rot + Anti	512 ± 137	619 ± 104	510 ± 169	622 ± 165

The data are averages of 10 independent homogenate preparations ± SD and expressed in pmol  $H_2O_2$ /min/mg protein. Experimental conditions like in the legends to Figs. 1, 2 and 3.

<sup>a</sup> Please note the substantial endogenous catalase-sensitive Amplex Red oxidation rate.

auranofin and DNCB to hippocampal slice cultures while monitoring superoxide and peroxide formation by microfluorimetry. Slice cultures were stained with the fluorescent free radical indicators MitoSox and  $H_2$ DCFDA. Although none of the indicators is completely selective for a certain radical, MitoSox was shown to be preferentially oxidized to ethidium by superoxide [18], whereas  $H_2$ DCFDA mainly reacts with peroxides forming the fluorescent DCF. Due to its mitochondrial accumulation MitoSox fluorescence was dotted, whereas DCF was homogeneously distributed in the cytosol of neurons and in putative glial cells (Fig. 5A). Interestingly microglial cells at the culture surface were rarely labeled with DCF at the beginning of the recording.

During the first minutes of recording fluorescence of MitoSox/DCF rose, likely due to the combination of laser illumination and the high  $pO_2$  of the recording chamber [19]. After reaching a peak within ~2 min, photo-bleaching dominated the fluorescence baseline. Bleaching of DCF fluorescence was more severe than that of MitoSox. Without addition of auranofin fluorescence decreased continuously following an initial rise for the whole duration of the experiment ( $n=7$ ). By contrast, application of auranofin resulted in a rise in DCF fluorescence (in 8 out of 9 slice cultures, Fig. 5B). The increase in DCF fluorescence was only accompanied by a small increase in MitoSox fluorescence (not shown), suggesting that the auranofin effect on DCF fluorescence is not due to an enhanced superoxide production, but as expected related to higher  $H_2O_2$  formation. Application of DNCB resulted also in a marked rise in DCF fluorescence in all slice cultures ( $n=6$ , data not shown).

Irrespective of which system of hydrogen peroxide removal was inhibited, DCF fluorescence showed the same heterogeneous distribution between different cell types. A few large stellate neurons in the stratum radiatum showed a massive increase in DCF-fluorescence, whereas the majority of the pyramidal cells were less affected by the inhibitors (Fig. 5A–C). Most remarkably, superficial microglial cells, as identified by their form and motility expressed a large increase in fluorescence, occasionally followed by disruption of the cell membrane and complete loss of the dye. Whether these differences reflect different metabolic rates or cell type specific differences in the antioxidant defense capacity remains to be elucidated. At higher magnification, cells intensely labeled by DCF revealed a fine web of filamentous structures, likely representing the mitochondrial network (Fig. 5D).

## 4. Discussion

In this work we estimated the relative role of the Trx2- and GSH-systems and catalase for hydrogen peroxide detoxification in different preparations from rat brain. For this we used the specific inhibitors



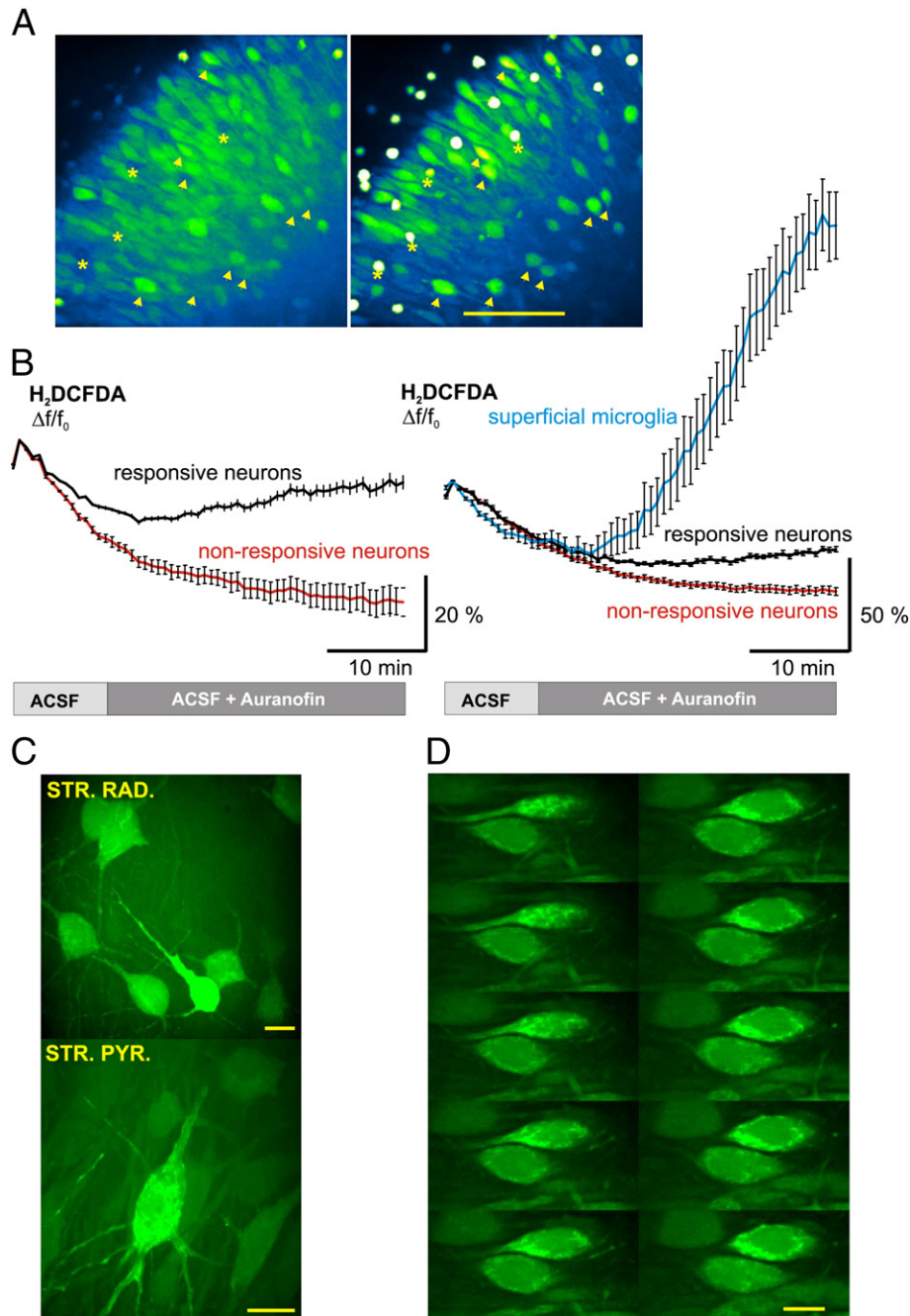


**Fig. 5.** Effects of auranofin on hydrogen peroxide formation in hippocampal slice cultures. (A) Representative image of CA3 region in a hippocampal slice culture stained with  $H_2DCFDA$ . The dye is homogeneously distributed at the beginning of the recording (left). At the end of the recording (right) fluorescence increased in a subpopulation of neurons (arrowheads) and in microglial cells (asterisks). Scale bar:  $50\ \mu m$ . (B) Time course of DCF fluorescence changes during auranofin application, responsive and non-responsive neurons (left) were distinguished based on the kinetics of the fluorescence bleaching curve. Massive fluorescence increase of fluorescence in superficial microglia as compared to neuronal changes in fluorescence (right). (C) Higher magnification image of neurons brightly labeled with DCF in the stratum radiatum (upper) and stratum pyramidale of CA3 region. Scale bar  $10\ \mu m$ . (D) Montage of the images taken at different focal planes ( $z = 0.8\ \mu m$ ) from a CA3 cell representing inhomogeneity in the cytosolic fluorescence. Note the presence of filamentous structures in the cytosol. Scale bar  $10\ \mu m$ .

of Trx2-system auranofin [6,20], of the GSH-system DNCB [20] as well as the catalase inhibitor aminotriazole [6]. Recent publications indicated a potentially important role of the Trx2-system for hydrogen peroxide utilization of brain mitochondria and heart mitochondria [6,20]. Here, we directly show that the Trx2-system contributes in isolated rat brain mitochondria to over 60% of the intramitochondrial hydrogen peroxide turnover. On the other hand the contribution of the GSH-system was, with about 20%, considerably lower. Interestingly, both the Trx2- and the GSH-system appear to detoxify preferentially mitochondrially produced  $H_2O_2$ , since the substantial endogenous hydrogen peroxide generation of hippocampal homogenates was

nearly unaffected by both auranofin and DNCB. That endogenous hydrogen peroxide generation of hippocampal homogenates might potentially originate from peroxisomes present in non-neuronal cell types.

On the other hand, the different location of individual sites of ROS generation by mitochondrial respiratory chain had apparently no influence on the speed of hydrogen peroxide detoxification. In the presence of  $\alpha$ -glycerophosphate and antimycin the superoxide is formed by complex III in the intermembrane space and is dismutated by intrinsic Cu, ZnSOD of the intermembrane space, or externally added Cu, ZnSOD. Here, the sites of hydrogen peroxide formation

and removal are different to the condition of succinate alone or glutamate + malate + rotenone, where the superoxide is formed by complex I in the matrix compartment and dismutated by matrix MnSOD. The absence of detectable differences in the auranofin and DNCB effects suggests therefore that the mitochondrial inner membrane does not create a considerable diffusion barrier for H<sub>2</sub>O<sub>2</sub>.

Imaging experiments of hippocampal slice cultures indicated substantial heterogeneity of hydrogen peroxide detoxification reactions between different cell types. Microglia and certain neurons (presumably mitochondria-rich interneurons) seem to depend to a high extent on hydrogen peroxide detoxification by the Trx2- and GSH-systems. Consequently, those cells are more susceptible against inhibitors of these systems.

The described high complexity and compartmentation of hydrogen peroxide detoxification reactions in the rat hippocampus are proposed to have a strong impact on ROS metabolism with important consequences for signaling and pathology.

### Acknowledgements

This work was supported by grants of the Deutsche Forschungsgemeinschaft (SFB TR3/D12), the DAAD exchange program Germany–Poland, and the BMBF (01GM0868) to WSK, the Hertie-Foundation to RK and the International PhD Projects Programme (MPD): ‘Neuro PhD’ operated within the ‘Innovative Economy’ Operational Programme 2007–2013, Priority axis 1: Research and development of new technologies to BA.

### References

- [1] A.P. Kudin, D. Malinska, W.S. Kunz, Sites of generation of reactive oxygen species in homogenates of brain tissue determined with the use of respiratory substrates and inhibitors, *Biochim. Biophys. Acta* 1777 (2008) 689–695.
- [2] M. Dynowski, G. Schaaf, D. Loque, O. Moran, U. Ludewig, Plant plasma membrane water channels conduct the signalling molecule H<sub>2</sub>O<sub>2</sub>, *Biochem. J.* 414 (2008) 53–61.
- [3] A.G. Cox, C.C. Winterbourn, M.B. Hampton, Mitochondrial peroxiredoxin involvement in antioxidant defence and redox signalling, *Biochem. J.* 425 (2009) 313–325.
- [4] S.G. Rhee, S.W. Kang, T.S. Chang, W. Jeong, K. Kim, Peroxiredoxin, a novel family of peroxidases, *IUBMB Life* 52 (2001) 35–41.
- [5] H. Imai, Y. Nakagawa, Biological significance of phospholipid hydroperoxide glutathione peroxidase (PHGPx, GPx4) in mammalian cells, *Free Radic. Biol. Med.* 34 (2003) 145–169.
- [6] D.A. Drechsel, M. Patel, Respiration-dependent H<sub>2</sub>O<sub>2</sub> removal in brain mitochondria via the thioredoxin/peroxiredoxin system, *J. Biol. Chem.* 285 (2010) 27850–27858.
- [7] R. Radi, J.F. Turrens, L.Y. Chang, K.M. Bush, J.D. Crapo, B.A. Freeman, Detection of catalase in rat heart mitochondria, *J. Biol. Chem.* 266 (1991) 22028–22034.
- [8] M. Salvi, V. Battaglia, A.M. Brunati, N. LaRocca, E. Tibaldi, P. Pietrangeli, L. Marcocci, B. Mondovì, C.A. Rossi, A. Toninello, Catalase takes part in rat liver mitochondria oxidative stress defense, *J. Biol. Chem.* 282 (2007) 24407–24415.
- [9] A.J. Kowaltowski, N.C. de Souza-Pinto, R.F. Castilho, A.E. Vercesi, Mitochondria and reactive oxygen species, *Free Radic. Biol. Med.* 47 (2009) 333–343.
- [10] M.P. Murphy, How mitochondria produce reactive oxygen species, *Biochem. J.* 417 (2009) 1–13.
- [11] D.F. Stowe, A.K. Camara, Mitochondrial reactive oxygen species production in excitable cells: modulators of mitochondrial and cell function, *Antioxid. Redox Signal.* 11 (2009) 1373–1414.
- [12] S. Ueda, H. Masutani, H. Nakamura, T. Tanaka, M. Ueno, J. Yodoi, Redox control of cell death, *Antioxid. Redox Signal.* 4 (2002) 405–414.
- [13] P.J. Halvey, W.H. Watson, J.M. Hansen, Y.M. Go, A. Samali, D.P. Jones, Compartmental oxidation of thiol–disulphide redox couples during epidermal growth factor signalling, *Biochem. J.* 386 (2005) 215–219.
- [14] J.M. Hansen, H. Zhang, D.P. Jones, Differential oxidation of thioredoxin-1, thioredoxin-2, and glutathione by metal ions, *Free Radic. Biol. Med.* 40 (2006) 138–145.
- [15] R.E. Rosenthal, F. Hamud, G. Fiskum, P.J. Varghese, S. Sharpe, Cerebral ischemia and reperfusion: prevention of brain mitochondrial injury by lidoflazine, *Cereb. Blood Flow Metab.* 7 (1987) 752–758.
- [16] A.P. Kudin, N.Y. Bimpong-Buta, S. Vielhaber, C.E. Elger, W.S. Kunz, Characterization of superoxide-producing sites in isolated brain mitochondria, *J. Biol. Chem.* 279 (2004) 4127–4135.
- [17] L. Stoppini, P.A. Buchs, D. Muller, A simple method for organotypic cultures of nervous tissue, *J. Neurosci. Methods* 37 (1991) 173–182.
- [18] K.M. Robinson, M.S. Janes, J.S. Beckman, The selective detection of mitochondrial superoxide by live cell imaging, *Nat. Protoc.* 3 (2008) 941–947.
- [19] R. Kovács, S. Schuchmann, S. Gabriel, O. Kann, J. Kardos, U. Heinemann, Free radical-mediated cell damage after experimental status epilepticus in hippocampal slice cultures, *J. Neurophysiol.* 88 (2002) 2909–2918.
- [20] B.A. Stanley, V. Sivakumar, S. Shi, I. McDonald, D. Lloyd, W.H. Watson, M.A. Aon, N. Paolucci, Thioredoxin reductase-2 is essential for keeping low levels of H(2)O(2) emission from isolated heart mitochondria, *J. Biol. Chem.* 286 (2011) 33669–33677.